

## Static structure analysis of EMU CR400AF high speed train's hollow axle using ansys workbench

Tito Syahril Sobarudin Izha Mahendra , Muhamad Fitri\*

\*Mechanical Engineering Study Program, Faculty of Engineering, Mercu Buana University, Indonesia. Jln. Raya Meruya Selatan No.1, West Jakarta, Indonesia

\*✉ [muhamad.fitri@mercubuana.ac.id](mailto:muhamad.fitri@mercubuana.ac.id)

Submitted: 09/06/2024

Revised: 01/07/2024

Accepted: 20/07/2024

**Abstract:** One of the important components in a train is the wheel axle part whose main function is to distribute the load on the train body to the wheels towards the rails. On conventional trains, train wheel axles still often have material failures in the form of cracks and even breaks. The wheel shaft used by conventional trains is solid while the one used in the fast train uses a hollow axle so that the risk is greater. To confirm and confirm the strength of the hollow axle structure, it is necessary to analyze the structure of the hollow axle when receiving static loading due to the load of the train body. The parameters measured are maximum stress, safety of factor, and maximum deformation. The analysis process is carried out using manual theoretical calculations and simulations with finite element methods using ANSYS Workbench software. In the theoretical calculation, the maximum stress value is 59.71 MPa and the safety factor value is 8.87, and the simulation results get a maximum stress of 62.02 MPa, a safety factor value of 8.54, and the maximum deformation that occurs is only 0.086mm. The difference from the theoretical calculation and simulation of the maximum stress and safety of the factor was 3.70% and 3.72%. Based on the results obtained, it can be concluded that the hollow axle is safe because the maximum stress < the material allowable voltage and the safety of factor (SF) value < the material standard value of 4,5.

**Keywords:** Static structure; hollow axle; ANSYS workbench

### 1. INTRODUCTION

The world's railway transportation modes are getting more rapid, one of which is high-speed trains [1]. High-speed train operations have been successfully carried out in Indonesia in 2023 which adopts high-speed trains from China, namely the EMU CR400AF series. High-speed trains are trains that have a speed of more than 200 km/h [2]. Generally, in conventional trains, the train shaft uses a solid shaft while this CR400AF EMU train uses a shaft that has a hole in it or is often called a hollow axle.

In conventional trains, the shaft still often has material failures in the form of cracks and even breaks, while in high-speed trains, hollow axles are used which have a hollow structure so that they can pose a greater risk [3]. Previous research that discussed the axle was the analysis of stress on the axle of the train carriage wheels using the FEA method with a maximum stress value at maximum load due to impact load due to bumpy wheels of 112.3 N/mm<sup>2</sup> and 109.4 N/mm<sup>2</sup>. These results are still safe because they do not exceed the permissible stress in the Von Mises failure theory, which is 225 N/mm<sup>2</sup> [4]. Failure Analysis of Axle with Finite Element Method Approach is also done by analyzing the torque moment against the shear force that occurs on the axle, the higher the torque moment given, the value of the safety factor decreases [5].

This hollow axle has an important role in supporting the heavy load of the car body. An axle is a machine component that functions to transmit power [6]. The main loading that a hollow axle receives is the static loading of the weight of the train itself and the weight of the passengers. The determination of the critical section of the wagon axle by considering dynamic, and safety factors study was used to confirm the effect of train load and speed based on variations in axle load, bending stress, moment and safety factor. The results of this study state that bending stress, moment, and safety factors increase linearly with train load [7]. Hollow axles must be designed according to applicable specifications, specifications, and regulations. To ensure the safety and quality of the structure of the



hollow axle, it is necessary to carry out a theoretical calculation process and design simulation testing in the form of static loading tests.

Static loading test simulations can be carried out using application software by providing loads on the hollow axle structure according to the actual load to be received [8]. Failure and characteristics of broken axles were analyzed using the finite element method to show stress concentration. Local stress is higher than bending stress on the axle surface which causes fatigue failure. The analysis method using Finite Element Analysis (FEA) is used to obtain a good design [9]. These calculations and simulations are expected to be a reference and ensure that the design of the hollow axle is safe to use. In the test simulation on a structure that uses a numerical approach, the finite element method is chosen as the approach to complete the simulation. The finite element method was chosen because of its ability to model various geometric forms of irregular structures, as well as its ability to handle non-linear aspects in terms of both geometry and materials [10]. Through static loading simulation, results can be obtained regarding the strength of the structure that can be supported by a component, so that it can calculate the strength of the hollow axle structure in bearing the weight of the train load and can transmit the traction power of the motor well.

Based on the description above, and the absence of force simulation on the hollow axle structure, the author aims to simulate the calculation of hollow axle strength using the ANSYS Workbench 2024 software application. The loading simulation carried out to test the strength of this hollow axle is a static loading test. With this simulation, results are obtained in the form of maximum stress values, maximum deformation, and safety factors that can determine the safety of the hollow axle design used in the EMU CR400AF high-speed train.

## 2. METHOD

### Literature study

The data used to conduct the research is the dimensional image data of the hollow axle trailer car on the EMU CR400AF train and the material data used is the EA4T material type. The hollow axle has a hole in the middle of the axle with a diameter of 30 mm. The second end of the hollow axle is a bearing with a diameter of 130 mm. The wheel seat section is assumed as a fixed support for the calculation which has a diameter of 191 mm. Figure 1 shows the shape and dimensions of the size of the hollow axle trailer car.

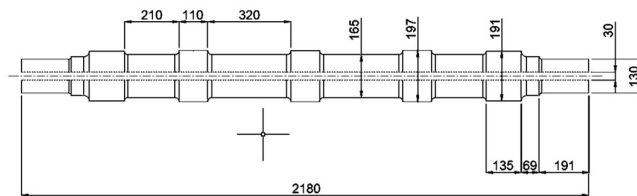


Figure 1. Dimension of the hollow axle trailer car.

The material used in the hollow axle components for EMU CR400AF trains is based on technical specifications according to the standard, namely using EA4T material [11]. The mechanical properties of the EA4T material are shown in Table 1 the following.

Table 1. Mechanical properties of EA4T material.

| No | Parameter                 | Unit | Reference Value |
|----|---------------------------|------|-----------------|
| 1  | Modulus elasticity        | MPa  | 209.726         |
| 2  | Yield Tensile Strength    | MPa  | 530             |
| 3  | Ultimate Tensile Strength | MPa  | 702             |
| 4  | Elongation                | %    | 12,2            |
| 5  | Poisson Ratio             | -    | 0,3             |

The data from the table above is the data from the mechanical properties of the EA4T material which will be used to perform calculations and enter the ANSYS Workbench software. The parameters that will be input into the ANSYS Workbench software are modulus of elasticity, tensile yield strength, ultimate tensile strength, elongation, and Poisson ratio.

In theoretical and simulation calculations, load data received by hollow axles is also required, so data on the weight of the train in the empty condition and full load is conditions contained in Table 2 the following.

Table 2. Train weight and passenger capacity of EMU CR400AF.

| Cars                        | TC1   | M2    | TP3   | M4    | M5    | TP6   | M7    | TC8   | Total  |
|-----------------------------|-------|-------|-------|-------|-------|-------|-------|-------|--------|
| Empty Load (t)              | 55,13 | 56,59 | 58,32 | 55,44 | 57,32 | 58,53 | 56,61 | 55,22 | 453,16 |
| Passenger capacity (people) | 37    | 90    | 90    | 80    | 75    | 90    | 90    | 49    | 601    |
| Total Passenger Weight (t)  | 2,96  | 7,2   | 7,2   | 6,4   | 6     | 7,2   | 7,2   | 3,92  | 48,08  |
| Total Load of Cars (t)      | 58,09 | 63,79 | 65,52 | 61,84 | 63,32 | 65,73 | 63,81 | 59,14 | 501,24 |

The data above will be used for calculations to determine the axle load that will be used in the calculation and simulation of the axle load of the motor car and the axle load of the trailer car. Strength is the ability of a material to withstand plastic deformation (stress without damage) [12]. Some materials such as structural steel and stainless steel have high tensile strength where the tensile strength and compressive strength are almost the same. Determine the strength of a material can be done by using tensile force, compressive force, or shear force [13].

Theoretical calculations on hollow axles

The steps for the manual calculation of the hollow axle are as follows:

a. Axle Load

The distribution of train loads to the hollow axle can be calculated using the axle load formula. Axle load is the load received by the rail track from one axle according to, the train classification as a plan for the analysis and planning of the dimensions of the rail track structure on high-speed trains adjusted to the needs of train operations.

$$\text{Axle Load} = \frac{\text{Total load of Cars}}{\text{Number of Axles}} \quad (1)$$

b. Force on Hollow axle

$$F = m \cdot g \quad (2)$$

Where:

M = mass

g = gravitational force

c. Free body diagram

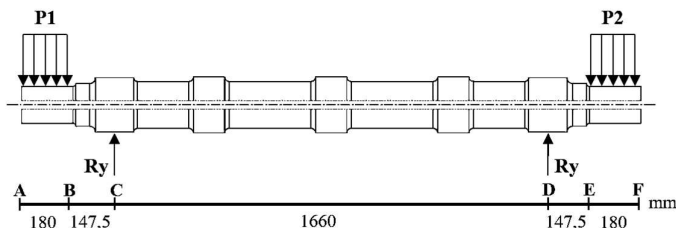


Figure 2. FBD of the hollow axle.

d. Moment of Inertia

The moment of inertia is a measure of the inertia of an object to rotate on its axis, the moment of inertia is also referred to as a quantity in rotational motion that is analogous to mass in translational motion [14]. Because the axle has rotational and translational motion, it cannot be separated from the moment of inertia. The moment of inertia can be interpreted as a derived quantity that is influenced by the radius of an object [15]. The moment of inertia can be calculated using the formula.

$$Ix_0 = Iy_0 = \frac{\pi(d_2^4 - d_1^4)}{64} \quad (3)$$

Where:

- $A$  = Cross Section Area
- $Ix_0$  = Moment Inertia  $X_0$
- $Iy_0$  = Moment Inertia  $Y_0$
- $\pi$  = Phi (3,14)
- $d_2$  = Outer Diameter
- $d_1$  = Inner Diameter

e. Von-Mises

Von Mises stress is a theory introduced by Huber and refined by von-mises and Heckly [16]. Von Mises stress is often used to determine the point of failure in a material. The failure criterion for von-mises occurs when the distortion reaches the same result as the failure test.

Principle stress:

$$\sigma_1, \sigma_2 = \frac{\sigma_x + \sigma_y}{2} \pm \sqrt{\left(\frac{\sigma_x - \sigma_y}{2}\right)^2 + \tau_{xy}^2} \quad (4)$$

Von-mises:

$$\sigma' = \sqrt{\frac{(\sigma_1 - \sigma_2)^2 + (\sigma_2 - \sigma_3)^2 + (\sigma_3 - \sigma_1)^2}{2}} \quad (5)$$

Where:

- $\sigma$  = Bending Stress
- $\sigma'$  = Von-mises
- $\tau$  = Shear Stress

f. Safety of Factor

The safety factor is a factor that shows the ability of a material to receive external loads. The determination of the safety factor is the result of a comparison of yield strength with maximum stress [17].

$$Safety\ Factor = \frac{Yield\ stren}{Maximum\ Stress} \quad (6)$$

The results of the calculation obtained will be compared with the standard in Table 3. The safety factor value provisions for this hollow axle are included in the criteria for known material conditions, but the load, stress, and environmental conditions are uncertain so they should not be less than 4.5.

Table 3. Value of the safety factor.

| No | Value Range | Remarks  |
|----|-------------|--|
| 1  | 1-1,5       | Controlled condition, working stress can be determined                                     |
| 2  | 1,5-2,0     | Materials whose value is already known   |
| 3  | 2,0-2,5     | Materials that operate on average with load limits are already known                       |
| 4  | 2,5-3,0     | Materials without being tested under average load and stress conditions                    |
| 5  | 3,0-4,5     | The materials are already known. Uncertain load, load stress, and environmental conditions |

ANSYS workbench software simulation on the hollow axle

Using ANSYS Workbench 2024 software will provide comparative data between manual calculation results and results obtained from software simulations. The results of the static structure software simulation process can be seen in Figure 3.

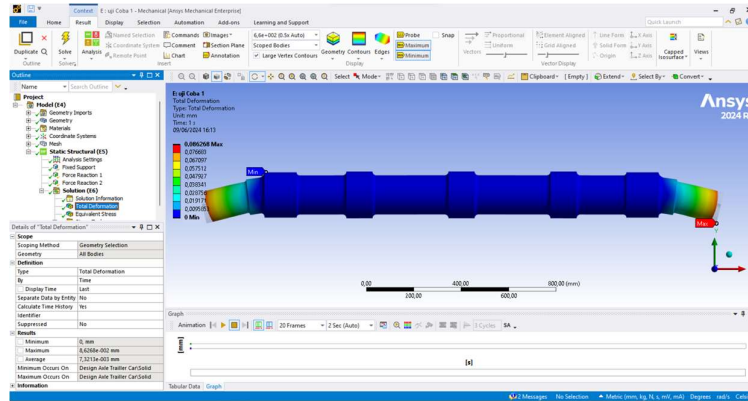


Figure 3. Static structure analysis with ANSYS workbench R1 2024.

### Data analysis

Quantitative mechanical data analysis is a method used when conducting studies related to numerical data. The data used in this analysis are manual calculation data and output data from ANSYS Workbench software. This analysis matched the results from the ANSYS Workbench software simulation that resulted in the maximum voltage value, maximum deformation value, and safety of factor. The data generated by the ANSYS Workbench software describes the output according to the results of the simulation without any manipulation. Data in the form of maximum voltage value, maximum deformation value, and safety of factor will be compared with EA4T material specification data and manual calculation data. The comparison was carried out to determine the suitability of the structure of the hollow axle in receiving the load from the train to ensure the strength of the structure and its safety.

## 3. RESULTS AND DISCUSSION

Theoretical calculation results on a hollow axle

### a. Axle load calculation

In this calculation, the loading reference used for hollow axle trailer cars is the largest total load of the trailer car, namely the TP6 train. So that the axle load of each car can be calculated. The axle load on the hollow axle trailer car is as follows:

$$\text{Axle Load} = \frac{\text{Total Load of Cars}}{\text{Number of Axle}} = \frac{65.730 \text{ kg}}{4} = 16.432,5 \text{ kg} \quad (7)$$

In the calculation and simulation, data on the load received by the hollow axle is also required. The calculation of the axle load based on the train weight data in empty and full load conditions can be calculated using the formula above and the results obtained are shown in Table 4. In this table, the largest load that will be used is 16,43 tons.

Table 1. Calculation results in axle load EMU CR400AF

| Cars                   | TC1   | M2    | TP3   | M4    | M5    | TP6          | M7    | TC8   | Total  |
|------------------------|-------|-------|-------|-------|-------|--------------|-------|-------|--------|
| Total Load of Cars (t) | 58,09 | 63,79 | 65,52 | 61,84 | 63,32 | 65,73        | 63,81 | 59,14 | 501,24 |
| Axle Load (t)          | 14,52 | 15,95 | 16,38 | 15,46 | 15,83 | <b>16,43</b> | 15,95 | 14,79 | -      |

### b. Force on the hollow axle

The axle load is divided into the right and left sides of the hollow axle end through the primary spring on the axle box. The largest force that will be calculated theoretically is the hollow axle trailer car. Each hollow axle receives a force, which is equal to the axle load received so that the amount of force on the hollow axle trailer car can be calculated.

$$F = m \cdot g = 164.32,5 \text{ kg} \cdot 9,8 \frac{\text{m}}{\text{s}^2} = 161.038,5 \text{ N} \quad (8)$$

c. Calculation of shear force and bending moment

For the calculation of shear force, the law of force equilibrium is used so that the Free Body Diagram (FBD) and Bending Moment Diagram (BMD) are obtained. At this stage, the maximum torque value of 13,688,315 N.mm is obtained as data to find the maximum tension value of the hollow axle in Figure 4 for the maximum bending stress value that occurs at points C and D, and the shear stress is evenly distributed from points A-C or D-F. because of the bending stress and shear force, the critical point is likely to be between B-C or D-E.

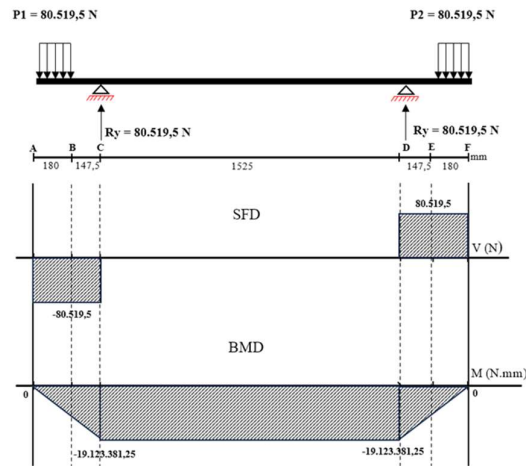


Figure 4. SFD and BMD hollow axle trailer car.

Based on the SFD and BMD diagrams above, the critical stress point is likely to be near points B and C or between points B and C. To better show the location of the point, the point must be cut into 3 parts and look like Figure 5.

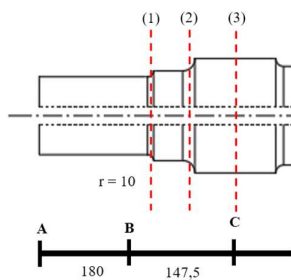


Figure 5. SFD dan BMD hollow axle trailer car.

d. Calculation of Von-Mises

In Figure 6 each section is selected 4 points to analyze the stress elements so that the stress elements can be obtained. The magnitude of the maximum bending moment and maximum shear force values on each element will be used to determine the von Mises stress.

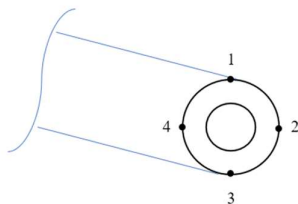


Figure 6. Cross-sectional properties on hollow axles.

Calculating the principal stress of section (1) at points 1 and points 3 of the hollow axle, it is known that  $d_1=30\text{mm}$ ,  $d_2=140$ , and  $M_{(1)} = 6,844,158 \text{ N.mm}$ .

- Maximum bending stress.

$$\sigma_x = \sigma_{max} = \frac{32 \times M}{\pi(d_2 - d_1)^3} = 52,38 \text{ MPa} \quad (9)$$

- Principle Stress:

$$\sigma_1, \sigma_2 = \frac{\sigma_x + \sigma_y}{2} \pm \sqrt{\left(\frac{\sigma_x - \sigma_y}{2}\right)^2 + \tau_{xy}^2} = \frac{\sigma_x}{2} \pm \frac{\sigma_x}{2} \quad (10)$$

$$\sigma_1 = \frac{\sigma_x}{2} + \frac{\sigma_x}{2} = 52,38 \text{ MPa}$$

$$\sigma_2 = \frac{\sigma_x}{2} - \frac{\sigma_x}{2} = 0 \text{ MPa}$$

- Von-Mises

$$\sigma' = \sqrt{\frac{(\sigma_1 - \sigma_2)^2 + (\sigma_2 - \sigma_3)^2 + (\sigma_3 - \sigma_1)^2}{2}} = 52,38 \text{ MPa} \quad (11)$$

Calculating the principal stress of section (1) at points 2 and 4 of the hollow axle, given  $d_1=30\text{mm}$ ,  $d_2=140$ , and  $V_{(1)}=80,519.5 \text{ N}$ .

- Maximum shear stress

$$\tau_{xy} = \tau_{max} = \frac{2V}{A} = 10,96 \text{ MPa} \quad (12)$$

- Principle Stress

$$\sigma_1, \sigma_2 = \frac{\sigma_x + \sigma_y}{2} \pm \sqrt{\left(\frac{\sigma_x - \sigma_y}{2}\right)^2 + \tau_{xy}^2} = \pm \tau_{xy}^2 \quad (13)$$

$$\sigma_1 = + \tau_{xy}^2 = 10,96 \text{ MPa}$$

$$\sigma_2 = - \tau_{xy}^2 = -10,96 \text{ MPa}$$

- Von-Mises

$$\sigma' = \sqrt{\frac{(\sigma_1 - \sigma_2)^2 + (\sigma_2 - \sigma_3)^2 + (\sigma_3 - \sigma_1)^2}{2}} = 18,98 \text{ MPa} \quad (14)$$

- e. Calculation of the safety of the factor

Calculating safety of factor on hollow axle trailer car.

$$Sf = \frac{\text{Yield strength}}{\text{Tegangan maksimum}} = \frac{530 \text{ Mpa}}{59,72 \text{ Mpa}} = 8,87 \quad (15)$$

Safety factor = 8,87

Safety factor > 4,5

- f. Results of Von Mises stress

Based on the formula and calculation steps that have been described, the principle stress and von Mises can also be obtained in sections (2) and (3). The results of these calculations are summarized in [Table 4](#). The largest von Mises stress is 59.72. The location of the von Mises stress can be called the critical point, which is in section (2).

[Table 4](#). Calculation results in axle load EMU CR400AF.

|                                  | Section (1) |            | Section (2)  |            | Section (3) |            |
|----------------------------------|-------------|------------|--------------|------------|-------------|------------|
| <b>1. Principle Stress (MPa)</b> | $\sigma_1$  | $\sigma_2$ | $\sigma_1$   | $\sigma_2$ | $\sigma_1$  | $\sigma_2$ |
| Points 1 & 3                     | 52,38       | 0          | 59,72        | 0          | 46,68       | 0          |
| Points 2 & 4                     | 10,96       | -10,96     | 8,30         | -8,30      | 5,76        | -5,76      |
| <b>2. Von-Mises (MPa)</b>        | $\sigma'$   |            | $\sigma'$    |            | $\sigma'$   |            |
| Points 1 & 3                     | 52,38       |            | <b>59,72</b> |            | 46,68       |            |
| Points 2 & 4                     | 18,98       |            | 14,38        |            | 9,98        |            |

## ANSYS Workbench 2024 software simulation results

### a. Maximum stress

The results of the Equivalent Von-Mises simulation process on the loading of hollow axles using ANSYS workbench 2024 R1 are the maximum stress, stress distribution, and location of the maximum stress that occurs. The maximum stress result produced by the simulation process due to receiving a load of 161,038.5 Newtons is 62.02 MPa. If the maximum stress value is less than the yield value of EA4T material, which is 530 MPa, then it can be concluded that the structure is safe. The location of the maximum stress on the hollow axle is located on the neck of the Axle shown in [Figure 7](#) and the stress distribution it leads to both pedestals is shown [Figure 8](#).

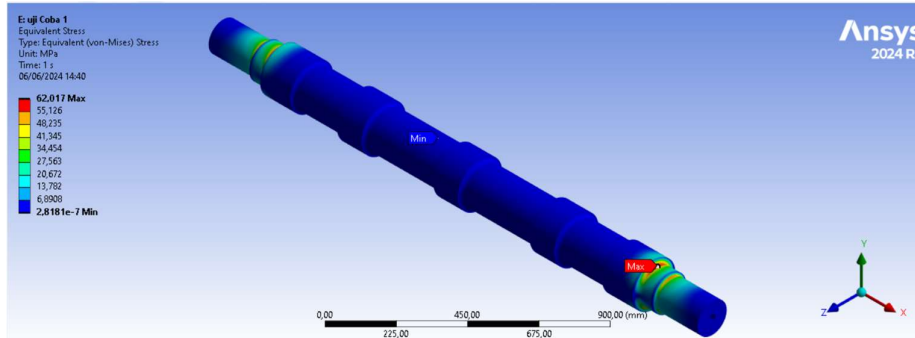


Figure 7. Equivalent von Mises simulation results.

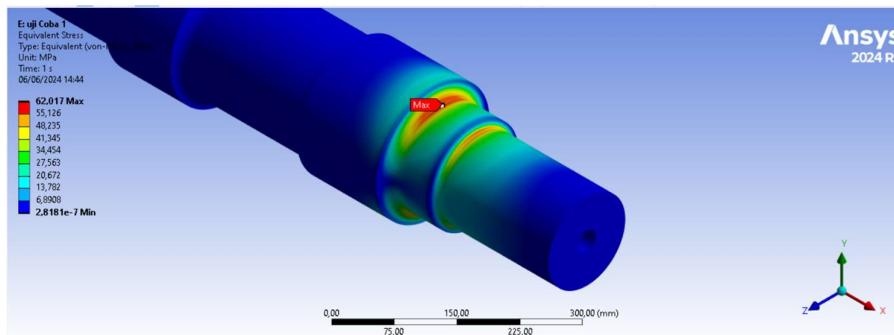


Figure 8. Maximum stress location.

### b. Maximum deformation

The result of the Total Deformation simulation process on the loading of hollow axles using Ansys workbench 2024 is a maximum deformation of 0.086 mm. As in [Figure 8](#) the location and distribution of the resulting deformation occurs at both ends of the hollow axle. Deformation that occurs is small so it is said to be safe and if the deformation that occurs is very large, it will interfere with the performance of other component structures. The greatest deformation lies at the end of the axle, precisely the axle box mount part shown in [Figure 9](#).

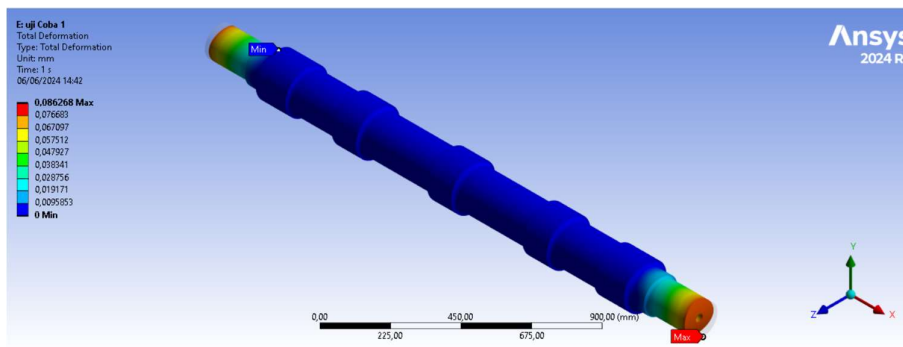


Figure 9. Total deformation simulation results.

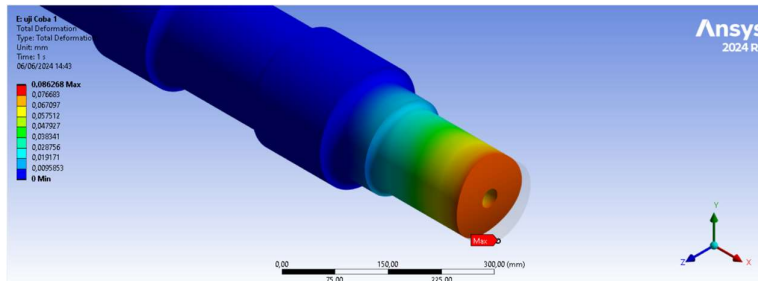


Figure 10. Location of maximum deformation.

c. Safety of factor

ANSYS Workbench 2024 R1 simulations can also demonstrate the safety of factor values that determine the ability of materials to accept external loads. The safety of factor value on this hollow axle is included in the criteria for known material conditions, but the load conditions, voltages, and surrounding environmental conditions are uncertain so it should not be less than 4,5. The location of the safety factor of the hollow axle can be seen in Figure 10 for the blue color is the largest value and the red color is the smallest value. The lowest safety factor value resulting from the simulation of the hollow axle trailer car is 8.54 as shown in Figure 11 which is located at the neck of the hollow axle. This result meets the standard requirements of the safety of factor value so that the hollow axle is safe when receiving static loads from the maximum load of the cars.

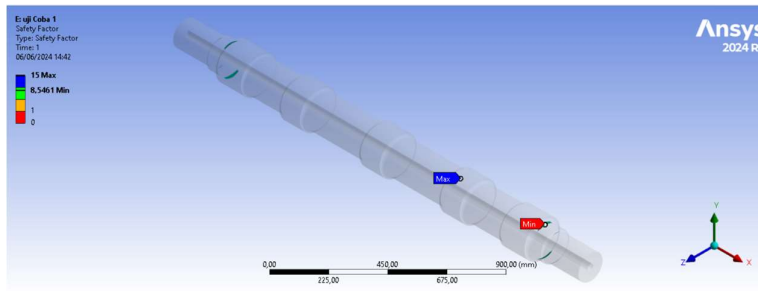


Figure 11. Safety of factor simulation results.

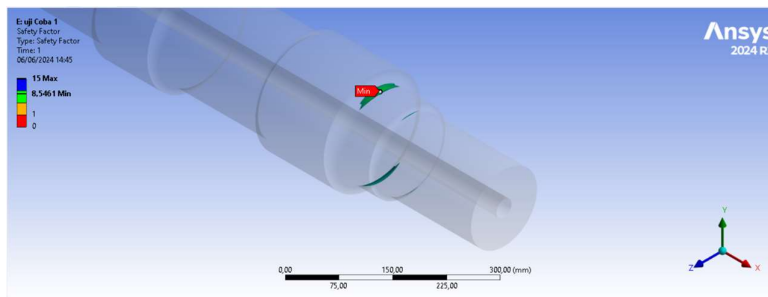


Figure 12. Location of minimum safety factor.

Analysis of calculation and simulation results

The results of the analysis of theoretical calculations manually and based on ANSYS Workbench 2024 R1 simulations can be shown in Table 5.

Table 5. Calculation and simulation results.

| No | Parameter        | Unit | Value Reference | Theoretical Calculations | Simulations Results | Gap (%) | Results |
|----|------------------|------|-----------------|--------------------------|---------------------|---------|---------|
| 1  | Maximum Stress   | MPa  | 530             | 59,72                    | 62,02               | 3,70    | Safe    |
| 2  | Safety of Factor | -    | >4,5            | 8,87                     | 8,54                | 3,72    | Safe    |

| No | Parameter           | Unit | Value Reference | Theoretical Calculations | Simulations Results | Gap (%) | Results |
|----|---------------------|------|-----------------|--------------------------|---------------------|---------|---------|
| 3  | Maximum Deformation | mm   | -               | -                        | 0,086               | -       | Safe    |

Table 5 it is known that the maximum stress obtained from the theoretical calculation results is 59.72 MPa while the simulation results of the ANSYS Workbench 2024 software test are 60.02 MPa. Then for the safety of factor values from calculations and simulations, the minimum values are 8,87 and 8.54. The simulation results also show that the maximum deformation on the hollow axle is 0.086 mm.

The comparison data of theoretical calculations and software simulations obtained a difference between the maximum stress and safety of factor values, which were 3,70% and 3,72%. The value of the percentage difference is said to be safe because it is not too significant, and the results of theoretical and simulated calculations are still within the safe limit because the maximum stress does not exceed the allowable stress of EA4T material of 530MPa and the safety of factor does not exceed 4,5.

#### 4. CONCLUSION

The conclusion was obtained from the results of the discussion analysis carried out with theoretical calculations and with ANSYS Workbench 2024 software simulations on the hollow axle structure of the EMU CR400AF high-speed train. The results of the theoretical calculation obtained a maximum stress value of 59,72 MPa and a safety factor value of 8,87. The results of the static loading simulation obtained a maximum stress value of 62.02 MPa and a safety factor value of 8,54. The highest maximum stress lies in the hollow axle neck. The maximum deformation that occurs on the hollow axle is 0.086 with the highest deformation location, namely at the ends of the hollow axle. The results of the comparative analysis of values from theoretical calculations and ANSYS Workbench 2024 R1 software simulations have a percentage difference of 3,70% for maximum voltage and 3,72% for safety of factor. The result was declared safe because the maximum stress and safety of the factor in the EA4T material did not exceed the permissible limit.

#### REFERENCE

- [1] M. Garmendia, C. Ribalaygua, and J. M. Ureña, "High speed rail: Implication for cities," *Cities*, vol. 29, no. SUPPL.2, pp. 26–28, 2012, doi: 10.1016/j.cities.2012.06.005.
- [2] Kementrian Perhubungan, "Penyelenggaraan kereta api kecepatan tinggi," 2022.
- [3] R. B. P. Sukoco, W. H. A. Putra, and S. H. Sujatanti, "Analisis Tegangan Pada Penegar Wrang Pelat Akibat Kemiringan Penegar Wrang Pelat," *J. Tek. ITS*, vol. 7, no. 2, 2019, doi: 10.12962/j23373539.v7i2.34475.
- [4] N. Supriyana and A. Kholidin, "Analisa Tegangan Poros Roda Gerbong Kereta Api Dengan Metode Elemen Hingga," *Simetris J. Tek. Mesin, Elektro dan Ilmu Komput.*, vol. 7, no. 2, p. 681, 2016, doi: 10.24176/simet.v7i2.781.
- [5] A. Rezaei, H. Masoudi, H. Z. Dizaji, and M. E. K. Ferdavani, "Modelling, analysis, and optimisation of the rear axle of cereal combine harvester under real loads using finite elements method," *J. Agric. Eng.*, vol. 54, no. 2, 2023, doi: 10.4081/jae.2023.1448.
- [6] M. Fitri and D. D. Saputra, "Simulasi Putaran Kritis pada Poros dengan Beban Alat Uji Putaran Kritis Menggunakan Software ANSYS," *J. UNITEK*, vol. 16, no. 1 SE-Articles, pp. 103–114, Jun. 2023, doi: 10.52072/unitek.v16i1.561.
- [7] F. Dikmen, M. Bayraktar, and R. Guclu, "Determination of critical section of wagon axle by considering dynamic and safety factors," *Alexandria Eng. J.*, vol. 58, no. 2, pp. 611–624, 2019, doi: 10.1016/j.aej.2019.05.010.
- [8] J. Arif, Pungkas Prayitno, and Halan Al Hafidh, "Analisis static pada aluminium 5052 dengan variasi sudut menggunakan solidworks," *TEKNOSAINS J. Sains, Teknol. dan Inform.*, vol. 10, no. 1, pp. 38–50, 2023, doi: 10.37373/tekno.v10i1.269.
- [9] H. Pranoto, M. Fitri, and A. F. Sudarma, "Analisis Statik Pelat Penyambung pada Ladder Frame Chassis Untuk Kendaraan Pedesaan Dengan Menggunakan Metode Elemen Hingga,"

- Rotasi*, vol. 23, no. 1, pp. 18–23, 2021.
- [10] F. Cannizzaro, B. Pantò, S. Caddemi, and I. Caliò, “A Discrete Macro-Element Method (DMEM) for the nonlinear structural assessment of masonry arches,” *Eng. Struct.*, vol. 168, pp. 243–256, 2018, doi: 10.1016/j.engstruct.2018.04.006.
- [11] Ingredion, “Technical Specification Technical Specification,” *Manual*, vol. 9, no. June, pp. 1–2, 2017.
- [12] Ž. Decker *et al.*, “Material’s Strength Analysis of the Coupling Node of Axle of the Truck Trailer,” *Materials (Basel)*, vol. 16, no. 9, 2023, doi: 10.3390/ma16093399.
- [13] Pramuko Ilmu Purboputro and Fransianto Setyo Aji, “Studi Age Hardening pada Struktur Mikro, Kekerasan dan Harga Impak Aluminium-Zink (Al-Zn) Hasil Cold Rolling dengan Reduksi 20%,” *JTTM J. Terap. Tek. Mesin*, vol. 3, no. 1, pp. 1–8, 2022, doi: 10.37373/jttm.v3i1.162.
- [14] C. Zhang, J. Miao, S. Tang, and G. He, “Moment of inertia measurement based on displacement sensor,” *Btaij*, vol. 10, no. 13, pp. 7500–7505, 2014.
- [15] S. Jumini and L. Muhliso, “Pengaruh Perbedaan Panjang Poros Suatu Benda terhadap Kecepatan Sudut Putar,” *Pros. Semin. Nas. Sains dan Pendidik. Sains VIII*, vol. 4, no. 1, pp. 133–138, 2013.
- [16] S. Krämer, S. Rothe, and S. Hartmann, “Homogeneous stress–strain states computed by 3D-stress algorithms of FE-codes: application to material parameter identification,” *Eng. Comput.*, vol. 31, no. 1, pp. 141–159, 2015, doi: 10.1007/s00366-013-0337-7.
- [17] L. A. N. Wibawa, K. Diharjo, W. W. Raharjo, and B. H. Jihad, “The effect of fillet radius and length of the thick-walled cylinder on von Mises stress and safety factor for rocket motor case,” *AIP Conf. Proc.*, vol. 2296, 2020, doi: 10.1063/5.0030329.